AIAA JOURNAL
Vol. 44, No. 2, February 2006

Technical Notes

TECHNICAL NOTES are short manuscripts describing new developments or important results of a preliminary nature. These Notes should not exceed 2500 words (where a figure or table counts as 200 words). Following informal review by the Editors, they may be published within a few months of the date of receipt. Style requirements are the same as for regular contributions (see inside back cover).

Effects of Aerodynamic Tabs on Screech Reduction of a Supersonic Jet

Mikiya Araki,* Kosuke Kuwabara,† Seiichi Shiga,‡ and Tomio Obokata§
Gunma University, Gunma 376-8515, Japan

I. Introduction

In the development of the next generation's supersonic transporter, environmental compliance is strongly required. In particular, a noise reduction system with a small loss is one of the key technologies for supersonic jet engines. From such supersonic jet engines, an underexpanded supersonic jet is exhausted, leading to strong screech radiation.[1–12]

A tab mounted at the nozzle exit is one of the most promising devices in screech reduction. The noise reduction performance and the mechanism were investigated by many researchers.[4–8] Kim et al.[9] and Araki et al.[10,11] investigated the effect of small jet injection on screech reduction of a supersonic jet, instead of mechanical tabs. In Refs. 9–11, it is shown that the screech can be removed completely. When practical applications of such aerodynamic tabs are considered, it is necessary to investigate 1) with how small a mass flow rate of the aerodynamic tab the screech can be removed and 2) what the criteria of the phenomena are. In the present study, the effects of the number, nozzle exit diameter, and mass flow rate of the aerodynamic tab on screech reduction of an underexpanded supersonic jet are investigated experimentally.

II. Experimental Setup and Procedure

A. Main and Secondary Jet Nozzles

Figure 1 shows a schematic of the nozzle exit. The compressed air for the underexpanded supersonic jet (main jet) is introduced to the nozzle through a settling section with honeycombs and screens. The total pressure is designated as P_{10}. The main jet nozzle is a converging round nozzle whose exit diameter $D = 8.0$ mm. At the exit of the main jet nozzle, a straight section (secondary jet flange) is attached, from which the secondary jets are injected. Note that the nozzle lip used is relatively large, which may affect the screech tone feedback loop.[1]

The compressed air for the aerodynamic tab (secondary jet) is introduced to the secondary jet flange, in which eight converging round nozzles are mounted with a pitch of 45 deg. The total pressure is designated as P_{20}. The exit diameter of the secondary jet nozzles is $1/8D$ and $1/16D$. The secondary jet is injected in the normal direction to the main jet. It is possible to choose the arbitrary nozzles from which the secondary jet is injected.

A cylindrical coordinate system is applied. The origin is set at the center of the main jet exit, and the x, r, and θ coordinates are set along the streamwise, radial, and circumferential directions. One of the secondary jet nozzles is set as the reference nozzle, and θ is set to be zero along the nozzle axis.

The pressure ratio of the main jet is set at 2.25, whose corresponding jet Mach number $M_j = 1.14$. In the present study, the pressure ratio is kept constant even when the secondary jets are injected. When the secondary jets are injected, the substantial exit area of the main jet is reduced due to the blockage effect. It is considered that the mass flow rate of the main jet is slightly reduced during the secondary jet injection. Table 1 shows the secondary jet conditions. The number of the secondary jets is two or four, with a pitch of 180 and 90 deg, respectively. The mass flow rate of the secondary jet is measured by a hot-wire flow meter, and each jet mass flow rate is varied from 0.25 to 4.0% of the main jet. In this estimation, the decrease in the main jet flow rate due to the secondary jet injection is not considered.

B. Measurements

In the sound pressure measurement, a piezoelectric pressure transducer (Piezotronics, 112A22) was used. The diaphragm diameter of the pressure transducer is 5.5 mm. The measured sound pressure is the average value over the diaphragm area. The natural frequency of the pressure transducer is about 250 kHz, which is large enough when compared with the jet noise frequency range in the present study. The sound pressure history is acquired with a digital

Table 1 Secondary jet conditions

Number	Nozzle exit diameter	Mass flow rate of each secondary jet, % of main jet
Without secondary jet (SJ)	——	0.0
2SJ	$1/8D$, $1/16D$	0.25–4.0
4SJ	$1/8D$, $1/16D$	0.25–4.0

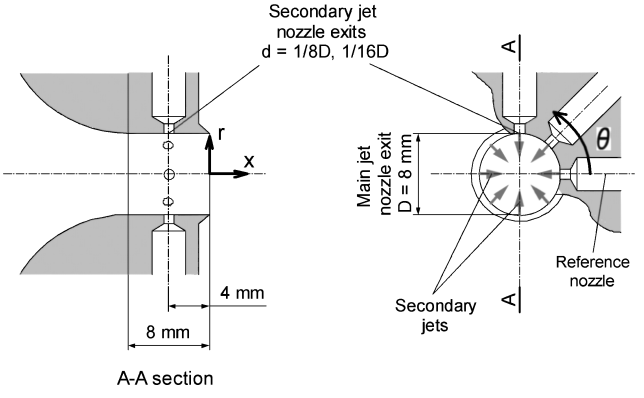

Fig. 1 Schematic of main and secondary jet nozzles.

Received 2 February 2005; revision received 30 August 2005; accepted for publication 26 September 2005.

*Research Associate, Department of Mechanical Engineering, 1-5-1, Tenjin-cho, Kiryu.
†Graduate School Student, Department of Mechanical Engineering, 1-5-1, Tenjin-cho, Kiryu.
‡Associate Professor, Department of Mechanical Engineering, 1-5-1, Tenjin-cho, Kiryu.
§Professor, Department of Mechanical Engineering, 1-5-1, Tenjin-cho, Kiryu.

oscilloscope at a sampling clock of 2.5 μs. The data are processed by fast Fourier transform, and the sound spectra are obtained. The measurement was carried out at the position of $x/D = 2.5$, $r/D = 5.0$, and $\theta = 0$ and 90 deg. The measurement position was determined so that the sound pressure level (SPL) near the third shock cell could be acquired because the screech SPL has the largest value around the third shock cell.[12] Note that the sound pressure measurements were carried out at a near field of the sound source.

In the Mie scattering method, a pulsed Nd: YAG laser (532 nm) was used. The thickness of the laser sheet at the measurement region is about 1 mm. Ethanol droplets were seeded into the main jet as the scattering particles. Ethanol vapor was mixed into the airflow through a mixing duct that is installed upstream of the main jet stagnation chamber. The ethanol vapor condenses into fine droplets due to the static temperature drop through the acceleration in the nozzle.[13] The mass fraction of the methanol was set to be about 3%. Scattered light was acquired with a charge-coupled device camera. Because the laser pulse duration is 12 ns, the acquired images are instantaneous.

In the total pressure measurement, a 0.3-mm o.d. pitot tube, mounted on a two-dimensional stage, was used. The pitot pressure distributions of the flow are obtained by scanning the stage. The pitot tube is scanned with a spacing of 0.2 mm ($r/D = 0.025$) in the r direction and 2.5 deg in the θ direction. The total pressure at each measurement position was calculated using Rayleigh's pitot tube formula.

III. Results and Discussion

A. SPL

Figure 2 shows typical results of the sound pressure measurements. Figures 2a, 2b, and 2c show the results for without a secondary jet (SJ), 2SJ,1/8D, and 2% at $\theta = 0$ deg; and 2SJ, 1/8D, and 2% at $\theta = 90$ deg, respectively. The horizontal axis indicates the frequency and the vertical axis the SPL. The frequency is nondimensionalized to a Strouhal number based on the nozzle exit diameter and exit velocity.

In Fig. 2a, an intensive peak of a screech is observed at a frequency of about 28 kHz. The screech SPL is about 130 dB. The corresponding overall SPL (OASPL) is 107.4 dB. In Figs. 2b and 2c, it is observed that the screech is completely removed and that the OASPL is reduced by about 1 dB. It is shown that the aerodynamic tab is effective in noise reduction in an underexpanded jet.[9–11] When

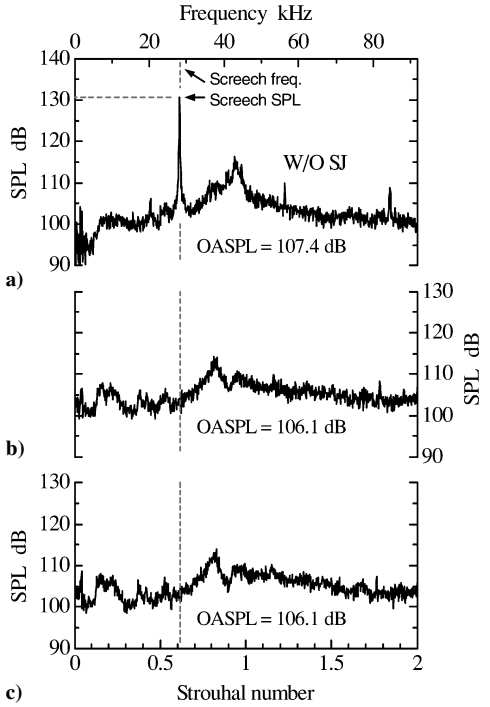

Fig. 2 SPL as function of frequency: a) without SJ, b) 2SJ, 1/8*D*, and 2% at $\theta = 0$ deg, and c) 2SJ, 1/8*D*, and 2% at $\theta = 90$ deg.

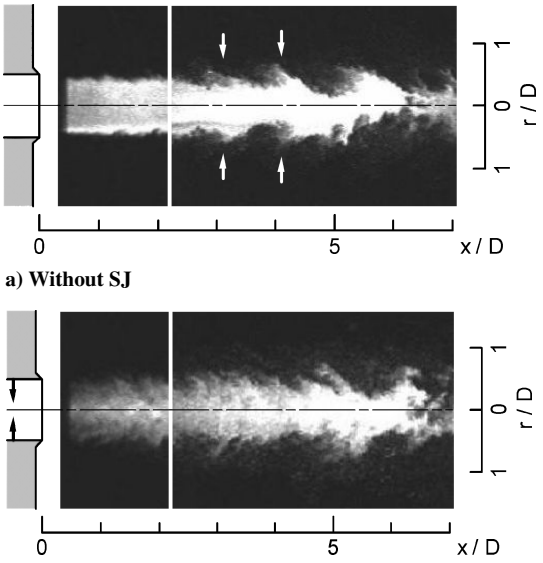

Fig. 3 Typical instantaneous Mie scattering images.

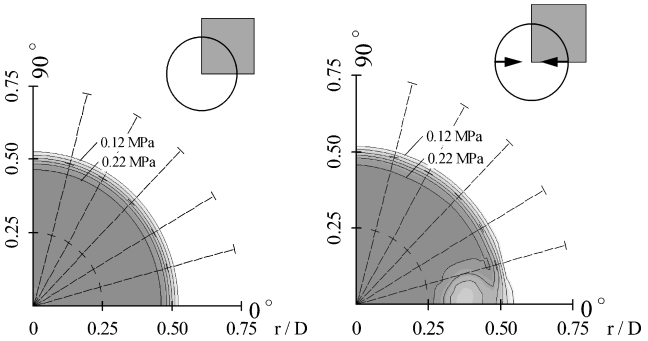

Fig. 4 Total pressure contours at $x/D = 0.25$.

Figs. 2b and 2c are compared, the sound spectra are similar. It is considered that the difference in the SPL distribution according to the measurement angle θ is relatively small. In the latter part of this Note, the data obtained at $\theta = 0$ deg are used as the representative SPL of the main jet.

B. Vortex Structures

Figure 3 shows typical instantaneous Mie scattering images. Along the x axis, the main jet cross section is shown. Two images that were obtained at different timings are connected at $x/D = 2.2$. Figures 3a and 3b show the images for without SJ and 2SJ,1/8D, and 2%, respectively. In Fig. 3a, it is shown that periodic large-scale structures (indicated with arrows) are formed in the shear layer between the main jet and ambient air. The vortices have an axisymmetric configuration, which has been observed in underexpanded jets oscillating in the toroidal mode.[1,2,4–8] In contrast, in Fig. 3b, the periodicity of the large structures are removed. It is considered that the SJ injection suppresses the periodicity of the large structure and that the shock/vortex feedback loop is removed.

C. Total Pressure Drop

Figure 4 shows the total pressure contours at $x/D = 0.25$. Figures 4a and 4b show the results for without SJ and 2SJ,1/8D, and 2%, respectively. The one-quarter area of the jet cross section is indicated. In Fig. 4a, an axisymmetric total pressure distribution is clearly observed. In contrast, in Fig. 4b, a pressure defect due to the SJ is observed. Because the SJ, which initially does not have the x-axis velocity component, penetrates into the main jet, the total pressure drop occurs locally. The magnitude of the total pressure

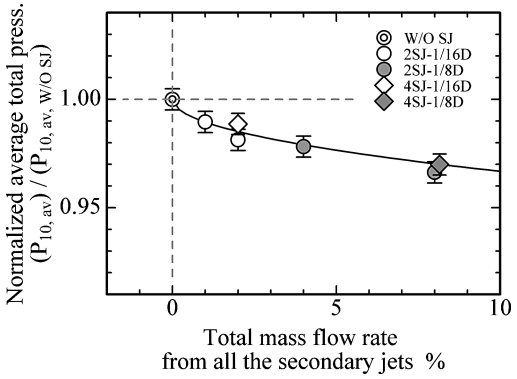

Fig. 5 Average total pressure of main jet as function of total mass flow rate from all SJs.

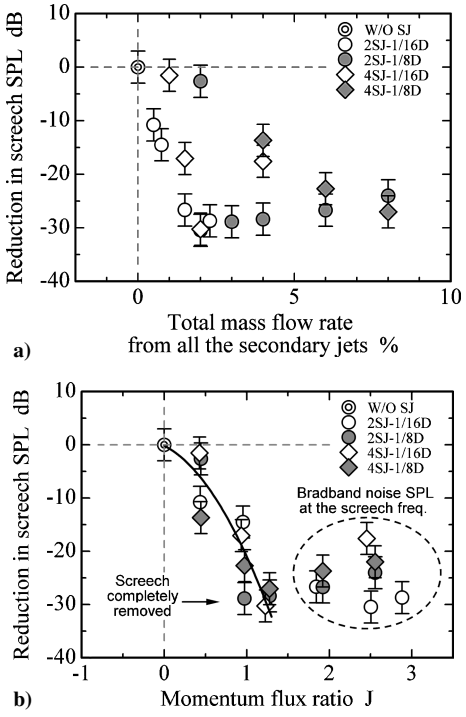

Fig. 6 Reduction in screech SPL as function of a) total mass flow rate and b) momentum flux ratio.

drop due to the secondary jet is estimated by averaging the total pressure distribution through the main jet cross section. The average total pressure of the main jet $P_{10,\mathrm{av}}$ is defined as follows:

$$P_{10,\mathrm{av}} = \iint P_{10,\mathrm{local}}(r,\theta)\,\mathrm{d}r\,\mathrm{d}\theta \Big/ A \tag{1}$$

where $P_{10,\mathrm{local}}(r,\theta)$ is the local total pressure calculated from the pitot pressure and A is the main jet exit area.

Figure 5 shows the average total pressure of the main jet $P_{10,\mathrm{av}}$ as a function of the total mass flow rate from all of the SJs. The vertical axis is normalized by the value for without SJ, and the error bar is estimated from the variation of the main jet total pressure P_{10}. It is shown that the average total pressure $P_{10,\mathrm{av}}$ decreases monotonously with the increase in the total mass flow rate of the SJs. It is natural that smaller mass flow rates are preferable from the viewpoint of the thrust losses in the engine.

D. Screech Reduction Performance

Figure 6 shows a reduction in the screech SPL with SJ conditions. Figures 6a and 6b show the effects of the total mass flow rate from all of the SJs, and the momentum flux ratio $J = (\rho u^2)_{\mathrm{SJ}}/(\rho u^2)_{\mathrm{MJ}}$, respectively. In Fig. 6a, it is shown that, when compared to the $1/8D$ nozzle, the screech SPL decreases more rapidly for the $1/16D$ nozzle, which indicates that screech reduction can be achieved with smaller losses in the total pressure. Both the screech and overall SPLs were reduced, at the maximum, by 30 and 6 dB, respectively, with the total mass flow rate of 2%, for 4SJ and $1/16D$. In Fig. 6b, it is shown that, though there is some scattering, the plots collapse onto one curve regardless of the number or exit diameter of the nozzle and that screech is completely removed at around $J = 1.2$. It is considered that the momentum flux ratio J is one of the most important criteria in the noise reduction performance of the aerodynamic tab, and it is believed that the penetration height of the SJ plays an important role in the phenomenon.

IV. Conclusions

Effects of the SJ from the nozzle wall on screech reduction of an underexpanded supersonic jet were investigated experimentally. The number, nozzle exit diameter, and mass flow rate of the SJ were varied, and the screech reduction performance was examined. When the SJ is used, the screech SPL decreases, which is possibly attributable to suppression of the periodicity of large structures in the underexpanded jet. The total pressure drop of the underexpanded jet increases monotonously with the increase in the total mass flow rate of the SJs. The screech SPL decreases with the increase in the momentum flux ratio between the SJs and main jets.

Acknowledgments

This research was funded by Grants-in-Aid for Scientific Research of the Ministry of Education, Culture, Sports, Science, and Technology of the Japanese government (15760595 and 17760634). The authors thank M. Arai, Y. Sone, and H. Nakamura of Gunma University for their help in the experiments.

References

[1]Raman, G., "Supersonic Jet Screech: Half-Century from Powell to the Present," *Journal of Sound and Vibration*, Vol. 225, No. 3, 1999, pp. 543–571.

[2]Powell, A., Umeda, Y., and Ishii, R., "Observations of the Oscillation Modes of Choked Circular Jets," *Journal of the Acoustical Society of America*, Vol. 92, No. 5, 1992, pp. 2823–2836.

[3]Umeda, Y., and Ishii, R., "Sound Sources of Screech Tone Radiated from Circular Supersonic Jet Oscillating in the Helical Mode," *International Journal of Aeroacoustics*, Vol. 1, No. 4, 2002, pp. 355–384.

[4]Ahuja, K. K., and Brown, W. H., "Shear Flow Control by Mechanical Tabs," AIAA Paper 89-0994, March 1989.

[5]Samimy, M., Zaman, K. B. M. Q., and Reeder, M. F., "Effect of Tabs on the Flow and Noise Field of an Axisymmetric Jet," *AIAA Journal*, Vol. 31, No. 4, 1993, pp. 609–619.

[6]Kobayashi, H., Oinuma, H., and Outa, E., "Supersonic Jet Noise Reduction Performance and Noise Reduction Mechanism of Tab Jet Noise Suppressor," *Acoustic Radiation and Wave Propagation*, ASME NCA-Vol. 17, 1994, pp. 149–163.

[7]Zaman, K. B. M. Q., "Spreading Characteristics of Compressible Jets from Nozzles of Various Gometries," *Journal of Fluid Mechanics*, Vol. 383, 1999, pp. 197–228.

[8]Outa, E., Kodama, R., and Kobayashi, H., "Computational Study of Supersonic Free Propulsion Jet Related with Screeching and Screech-Free Structures," *Proceedings the 16th International Symposium on Airbreathing Engines (ISABE 2003)* [CD-ROM], AIAA, Reston, VA, 2003.

[9]Kim, J. H., Kim, J. H., and Yoo, J. Y., "Noise Reduction in a Non-Ideally Expanded Round Jet via Steady Blowing," AIAA Paper 2003-1202, Jan. 2003.

[10]Araki, M., Kuwabara, K., Obokata, T., Ishima, T., and Shiga, S., "Effects of Side Jets on Noise Reduction of a Supersonic Jet," *Proceedings of 17th International Symposium on Airbreathing Engines (ISOABE 2005)* [CD-ROM], AIAA, Reston, VA, 2005.

[11]Araki, M., Kuwabara, K., Arai, M., Ishima, T., Shiga, S., and Obokata, T., "Noise Reduction of a Supersonic Jet Using Gas Injection from a Nozzle Wall," *Transactions of the Japan Society of Mechanical Engineers*, Vol. 71, No. 707, 2005, pp. 1798–1805 (in Japanese).

[12]Panda, J., "An Experimental Investigation of Screech Noise Generation," *Journal of Fluid Mechanics,* Vol. 378, 1999, pp. 71–96.

[13]Haimovitch, Y., Gartenberg, E., and Roberts, A. S., Jr., "Effects of Internal Nozzle Geometry on Compression-Ramp Mixing in Supersonic Flow," *AIAA Journal*, Vol. 35, No. 4, 1997, pp. 663–670.

C. Bailly
Associate Editor